Utah State University

From the SelectedWorks of Susanne U. Janecke

January 1, 2003

Extensional folds associated with Paleogene detachment faults in SE part of the Salmon basin

Susanne U. Janecke, *Utah State University*
J. C. Blankenau

Available at: https://works.bepress.com/susanne_janecke/38/

EXTENSIONAL FOLDS ASSOCIATED WITH PALEOGENE DETACHMENT FAULTS IN SE PART OF THE SALMON BASIN

SUSANNE U. JANECKE, and **JAMES J. BLANKENAU**†; Department of Geology, Utah State University, Logan UT, 84322-4505* sjanecke@cc.usu.edu and jblankenau@kleinfelder.com

present address: †Kleinfelder, 2677 East Parley's Way, Salt Lake City, UT 84109-1617

ABSTRACT

The southeast part of the Salmon basin of east-central Idaho is a complex east-dipping half graben that formed above several strands of a detachment fault and contains many extensional folds. The basin contains several unconformity-bounded sequences of Tertiary volcanic, alluvial fan, lacustrine, and fluvial deposits. From oldest to youngest these are the Challis Volcanic Group, Tendoy beds (new name), Sacagawea beds (new name), and Quaternary-Tertiary deposits. Cross-cutting relationships and angular unconformities show that the Salmon basin experienced several phases of extension, and that it lies in the core of a narrow Eocene to Oligocene rift zone. This trip examines the three-dimensional evolution of the basin during the major phases of extension and basin formation, the Eocene to Oligocene (?) Tendoy phase, Lemhi Pass phase, and the younger Sacagawea phases. Extensional folds are common, and form interference patterns due to a major period of cross-faulting that interrupted an otherwise simple history of ENE-WSW extension on the Salmon basin detachment fault and its predecessor, the Agency-Yearian fault. Slip was top to WSW and altogether resulted in more than 8-9 km of horizontal extension.

The Tendoy phase resulted in the formation of a WSW-dipping Agency-Yearian fault with two ramps and two flats, large overlying fault-bend folds, and deposition of the Tendoy beds in a strongly partitioned supradetachment basin. Faults and faults of the Tendoy phase trend N to NE but were reoriented during younger deformation. Facies of growth strata and megabreccia deposits in the subbasins indicate that the extensional folds produced considerable topography within the supradetachment basin. Subsequent slip on the SSW-dipping Lemhi Pass listric normal fault folded the preexisting subbasins about a SE-trending rollover anticline. The resulting interference between folds and normal faults of different orientations produced structural domes and basins. Sedimentation resumed and the basin continued to develop during the Sacagawea phase of deformation, after the disruption and reorientation of the Lemhi Pass fault phase had subsided. Slip on the WSW-dipping Salmon basin detachment fault expanded the NE-dipping Sacagawea supradetachment

Janecke, S. U., and Blankenau, J.C., 2003, Extensional folds associated with Paleogene detachment faults in SE part of the Salmon basin: Northwest Geology, v. 32, p. 51-73.

basin into the footwall of the older, faulted and folded Tendoy supradetachment basin, generated a rollover monocline and resulted in the deposition of the Sacagawea conglomerate beds. Limited geochronologic data show that extensional deformation was late-middle Eocene to Oligocene age but may have continue into early Miocene time.

The Salmon basin detachment fault is a regional detachment based on its >60 km lateral extent and low dip angle (~10-15°). This major fault is superimposed on preexisting structural culminations of the western reaches of the Sevier fold-and-thrust belt. The culminations had been denuded of their Mesozoic, Paleozoic and youngest part of the Belt succession prior to middle Eocene Challis volcanism and were the headwaters of large erosive rivers from late Cretaceous (?) to middle Eocene time.

INTRODUCTION

This field trip provides an overview of some of the key characteristics of the southeast part of the Salmon supradetachment basin (Fig. 1). This Eocene to early Miocene (?) basin formed in the hanging wall of the Salmon detachment fault, along the southwest front of the Beaverhead Range. It is of particular interest for the numerous, overlapping, large, and well developed extensional folds that deform the syn-rift deposits and underlying volcanic and metasedimentary rocks. Several lines of evidence show that the extensional folds partitioned the supradetachment basin into distinct subbasins on either side of a large rollover anticline (Fig. 2). The main subbasin was occupied by a lake in the Tendoy area (west of the anticline) whereas a diverse assemblage of sedimentary deposits including braided stream and rock avalanche deposits, occupied a smaller subbasin east of the Agency anticline.

REGIONAL SETTING

The Salmon supradetachment basin is just one example of an Eocene-early Miocene extensional basins in east-central Idaho and western Montana (Fields et al, 1985; Janecke, 1994, 1995; VanDenburg et al., 1998). Other supradetachment basins formed during this same middle Eocene-early Miocene interval include the Horse Prairie, Grasshopper, Medicine Lodge, Big Hole, Muddy Creek and Nicholia Creek basins (Fig. 3). These basins all contain lacustrine deposits and in most were occupied by large, locally long-lived lakes (Harrison, 1985; M'Gonigle et al., 1991; M'Gonigle and Dalrymple, 1993; Blankenau, 1999; Janecke et al., 1999; Kickham, 2002; Matoush, 2002). Coeval extensional basins in east-central Idaho lack lacustrine facies (Janecke, 1994) despite their apparently more humid climate and higher paleoelevations (Axelrod, 1968 and 1998). Lakes formed where east-flowing river systems were blocked by fault blocks beneath the Salmon basin, and Muddy-Grasshopper detachment faults. At higher elevations, to the west, smaller, less laterally continuous and less interconnected normal faults were defeated by upland streams, and external drainage was maintained during extension.

East-tilted basins in figure 3 formed above listric and low-angle normal faults of regional extent, and thus represent supradetachment basins. The single west-tilted basin, the very large and

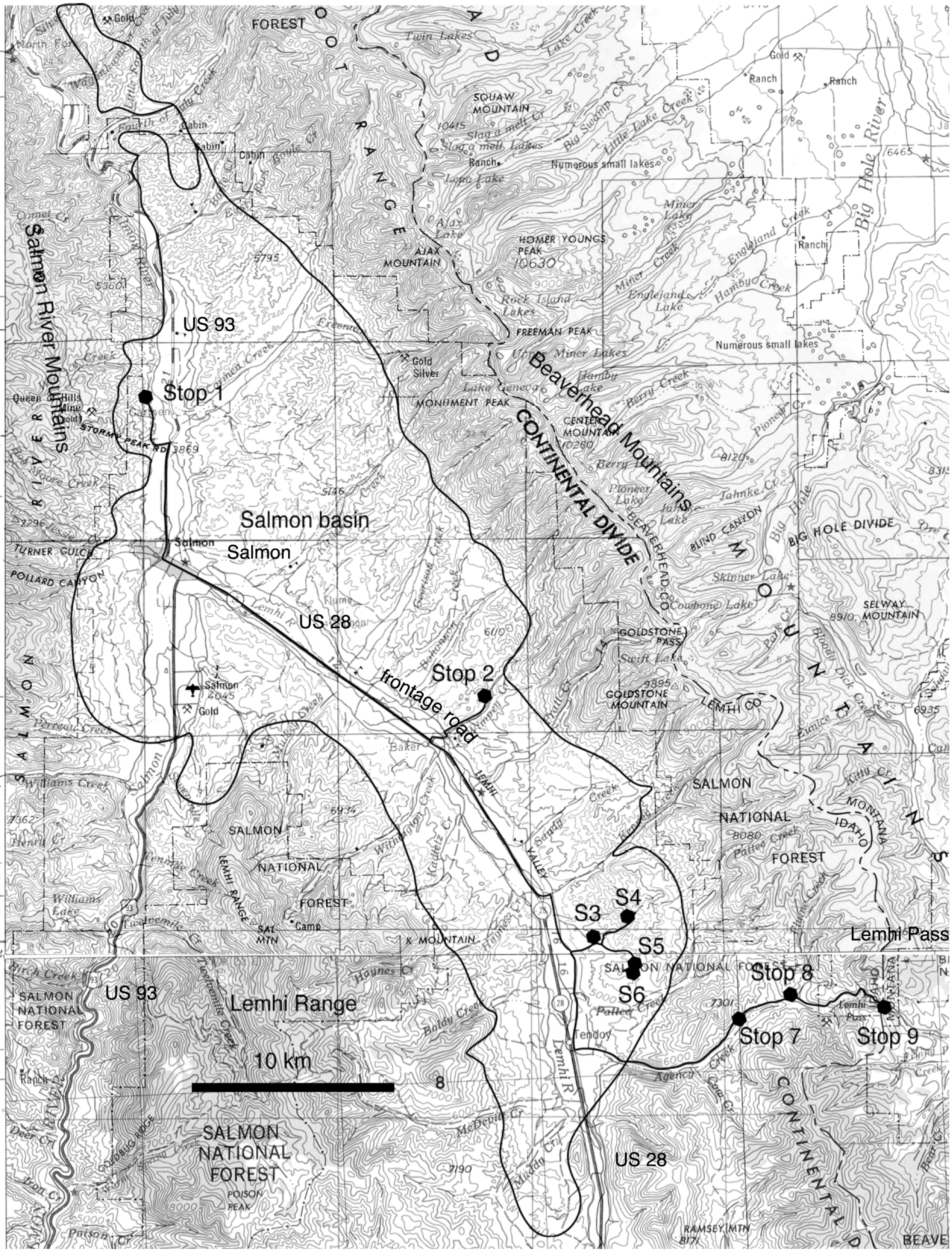

Figure 1. Topographic map of the Salmon basin showing field trip stops.

mostly buried Big Hole basin, lies in the hanging wall of a newly identified metamorphic core complex in the Anaconda-Pintlar ranges along its

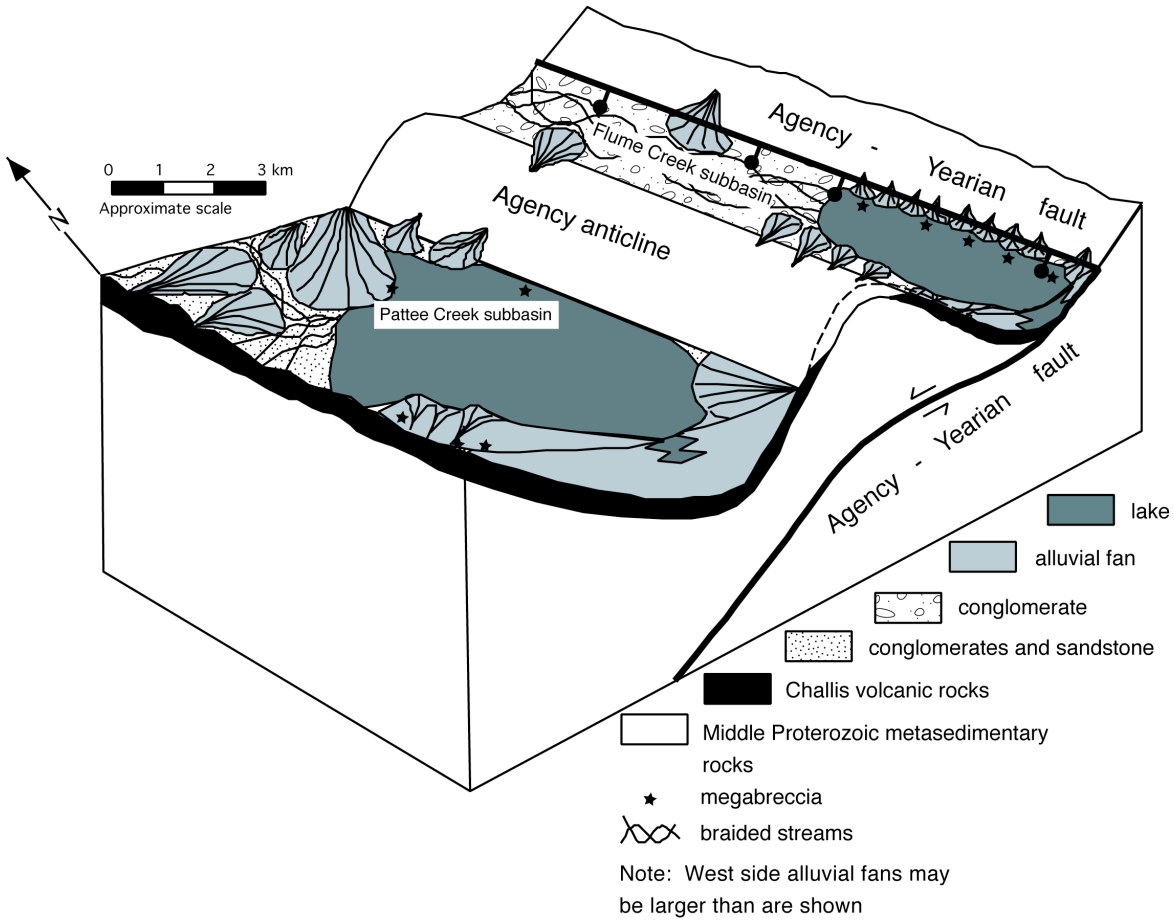

Figure 2. Block diagram illustrating the paleogeography during deposition of the Tendoy beds. Note that the Agency anticline, above a ramp-flat pair in the underlying Agency-Yearian detachment fault, segmented the basin into the Pattee Creek and Flume Creek subbasins. A large lake occupied the center of the Pattee Creek basin and alluvial fans carried quartzose debris flowed directly out into the lake from steep mountain fronts. The Flume Creek subbasin had significant volcanic material in its source terrain and braided streams flowed along the axis of this narrow subbasin.

northwest margin (O'Neill et al., 2002) but the relationship between the Big Hole basin and the apparently older metamorphic core complex is uncertain. Farther east, unextended terrain in the footwall of the
Muddy-Grasshopper normal fault was the site of deposition for the tectonically quiescent Renova Formation (Janecke, 1994). The Sage Creek basin was part of this footwall-flexure basin (Fig. 3).

The Salmon basin is a large intermontane basin in the northern Rocky Mountains that is superimposed on a series of large structural culminations that brings Middle Proterozoic metasedimentary rocks of the Belt basin and its equivalents to the surface. Most of the structural relief on these culminations developed in the late Mesozoic to early Tertiary Sevier orogeny (e.g., Tysdal, 2002) but some relief could be older. The culmination has been interpreted as a paleohigh dating back to Precambrian and early Paleozoic times (Armstrong, 1975; Ruppel, 1975; Burchfiel et al., 1992) and as a single (Skipp, 1987) or multiple (Janecke et al., 2000) structural culmination(s) of the Sevier fold-and-thrust belt. Paleozoic rocks are preserved only on the flanks of the paleohigh (Janecke et al., 2000), and are exposed 4.5 km south of the study area along Hayden Creek (Anderson, 1956) and along Reese Creek (Staatz, 1979; Evans and Green, 2003). Mesozoic, Paleozoic and some Mesoproterozoic rocks were eroded from the thrust-related culminations before middle Eocene volcanism (Rodgers and Janecke, 1992 and Janecke et al., 2000).

Erosion of the culminations in the Salmon area exposed a distinctive Mesoproterozoic rapakivi granite (Fig. 4), what is confined to the Salmon River Mountains west of the Salmon basin. The granite invaded Precambrian quartzites and meta-argillites of the Lemhi Group (Anderson, 1956) and the Yellowjacket Formation (Ruppel, 1975; Ruppel et al., 1993) 1370 Ma (Evans and Zartman, 1990; Doughty and Chamberlain, 1996). Clasts derived from the rapakivi granite occur locally in paleovalleys in the southeast part of the Salmon basin and in adjacent parts of southwest Montana, and help to delineate a paleovalley of late Mesozoic to middle Eocene age (Janecke et al., 2000) (see below). The relationship between the structural culminations and the Cretaceous-early Tertiary Idaho batholith, which surrounds the Salmon basin on the west and north, is unclear (Fig. 4).

The Salmon basin overlies an older, southeast-draining paleovalley. This paleovalley was initiated during the Sevier orogeny and was later filled with Eocene river gravels and volcanic rocks (Janecke et al., 2000). We will examine a distinctive ashflow tuff that filled this paleovalley. It flowed ESE through the area of Lemhi Pass, carried boulder gravels and funneled a distinctive ashflow tuff for >85 km downstream into southwest Montana. Structural culminations in the greater Salmon area were the ultimate source of the large volumes of coarse sediment that were carried through the paleovalley into the foreland basin in Cretaceous to early Tertiary time (Ryder and Scholten, 1973). Longitudinal transport within the foreland basin eventually moved this sediment over 250 km into northwest

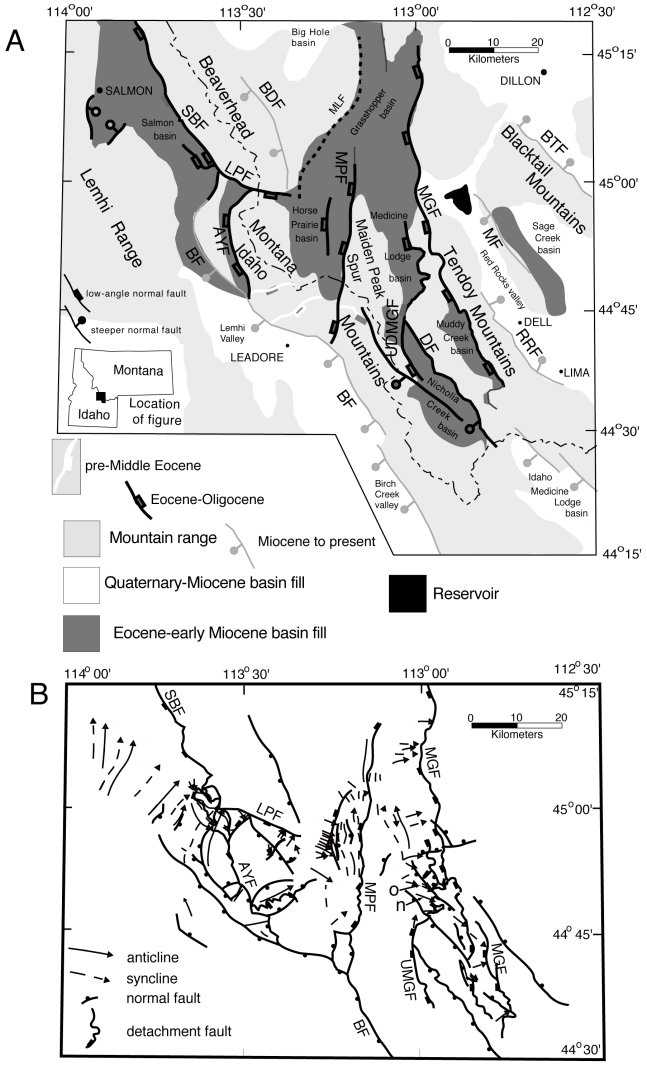

Figure 3. A) Rift basins of greater Salmon area. Map displays the geographic setting of the study area, shows some of the larger normal faults in the region and locations of supradetachment basins. Basins with predominately Paleogene basin fill are distinguished from basins with mostly Miocene to Quaternary basin fill. The age of the basin fill in the southern Big Hole basin is not known. The Sage Creek basin was east of the zone of active extension during the Paleogene (Janecke, 1994). Abbreviations: AYF = Agency-Yearian fault; BF = Beaverhead fault; BDF = Bloody Dick Creek fault; BTF = Blacktail fault; DF = Deadman fault; LPF = Lemhi Pass fault; MF = Monument Hills fault zone; MGF = Muddy-Grasshopper detachment fault; MLF = Meriwether Lewis fault; MPF = Maiden Peak fault; RRF = Red Rocks fault; SBF = Salmon basin detachment fault; and UDMGF = upper detachment fault of the Muddy-Grasshopper detachment fault system. Figure modified from Janecke et al. (2001). B) Simplified map showing extensional folds and normal faults in the region. From Janecke et al. (1998).

Wyoming (Lindsey, 1972; Ryder and Scholten, 1973; Janecke et al., 2000).). Table 1 outlines the geologic history of this area.

TABLE 1:
OUTLINE OF GEOLOGIC HISTORY OF SW MONTANA AND EASTERN IDAHO

Archean and Paleoproterozoic: The oldest rocks are Archean to earliest Proterozoic gneisses and metasedimentary rocks. This basement is exposed in western Montana and may extend beneath the Belt basin. New work by Foster et al. (2002) suggests that Paleo-Proterozoic rocks are present beneath the Belt basin at this latitude and that the west edge of the Wyoming province lies to the east.

1450 to 1400 Ma: Formation of the Belt rift basin with rift margin east of us in southwest Montana. Ten to 15 km of clastic rocks are deposited (ages of Evans et al., 2000)

1370 Ma: Mafic magmas and rapakivi porphyritic granites invade the Belt

basin. Some shearing follows (Evans and Zartman, 1990; Dougherty and Chamberlain, 1996).

850 to 900 Ma: Huge meteorite impact near the eastern margin of the Belt rift basin in the Beaverhead Mountains (Hargraves et al., 1990).

Neoproterozoic: Rifting of a continental mass from western North America in latest Proterozoic time (e.g. Moores, 1991; Karlstrom et al., 1999; Sears and Price, 2000).

Neoproterozoic to Ordovician: Begin deposition of cratonal to miogeoclinal sedimentary sequence. In many areas south of Salmon, Idaho, Ordovician rocks are the oldest miogeoclinal deposits deposited on the Salmon River arch. Deposition continues with interruptions into the Jurassic time. Youngest sedimentary rocks preserved nearby are Triassic (Bond, 1978).

Cretaceous (?): Initiate the Sevier fold-and-thrust belt. Synorogenic deposits shed from the thrust belt first appear in the lower Cretaceous Kootenai Formation, and persists during deposition of the overlying Blackleaf Formation and Cretaceous to Lower Tertiary Beaverhead Group (sandstone and conglomerate). Rivers carried sediment toward the foreland basin farther to the east. Structural culminations develop in the greater Salmon area (Skipp, 1987; Janecke et al., 2000; Tysdal, 2002) (Fig. 4). Idaho batholith invaded the western part of the fold-and-thrust belt in late Cretaceous time.

Early Tertiary: End of shortening and begin a long history of extension. Oldest normal faults dip SW and may have formed during Sevier shortening (Tysdal and Moye, 1996; Tysdal, 1996a, 1996b, 2002; VanDenburg et al., 1998). Earliest extension began before ~50-45 Ma Challis volcanism. Many phases of extension followed, and continued to the present (Janecke, 1992; Sears and Fritz, 1998; VanDenburg et al., 1998; Janecke et al. 2001) (Fig. 5).

Middle Eocene (50 to 45 Ma): Challis volcanic field develops in the western part of the area. Very intense volcanic activity during a short period of time. More intrusive activity in the Idaho batholith at this time. Ancient rivers, which probably initiated during Sevier thrusting, were carrying sediment to the east at beginning of volcanism. Paleorivers are overwhelmed and valleys were filled by the volcanic rocks by the end of the volcanism (Janecke et al., 2000). From the Bitterroot Range northward, a phase of extreme extension begins during Challis magmatism and several metamorphic core complexes form (Foster and Fanning, 1997). South of the Bitterroot Range, in central Idaho, more modest extension along NE-striking, high-angle normal faults develops during Challis volcanism and the large-magnitude extension largely post-dates volcanism (Janecke et al., 2001).

Late Eocene to early Miocene: Main phase of extension in the Salmon area was probably during the Eocene to Oligocene but deformation persisted into Early Miocene time in some adjacent areas (extension from 46 to ~20? Ma). Supradetachment basins may have initiated during terminal phases of Challis magmatism. Many E-tilted half graben formed in a narrow N-S-trending rift zone. Detachment faults and extensional folds form. Supradetachment basins in the region include the Grasshopper, Muddy Creek, Horse Prairie, Medicine Lodge, Nicholia Creek, and Salmon basins (Fig. 3).

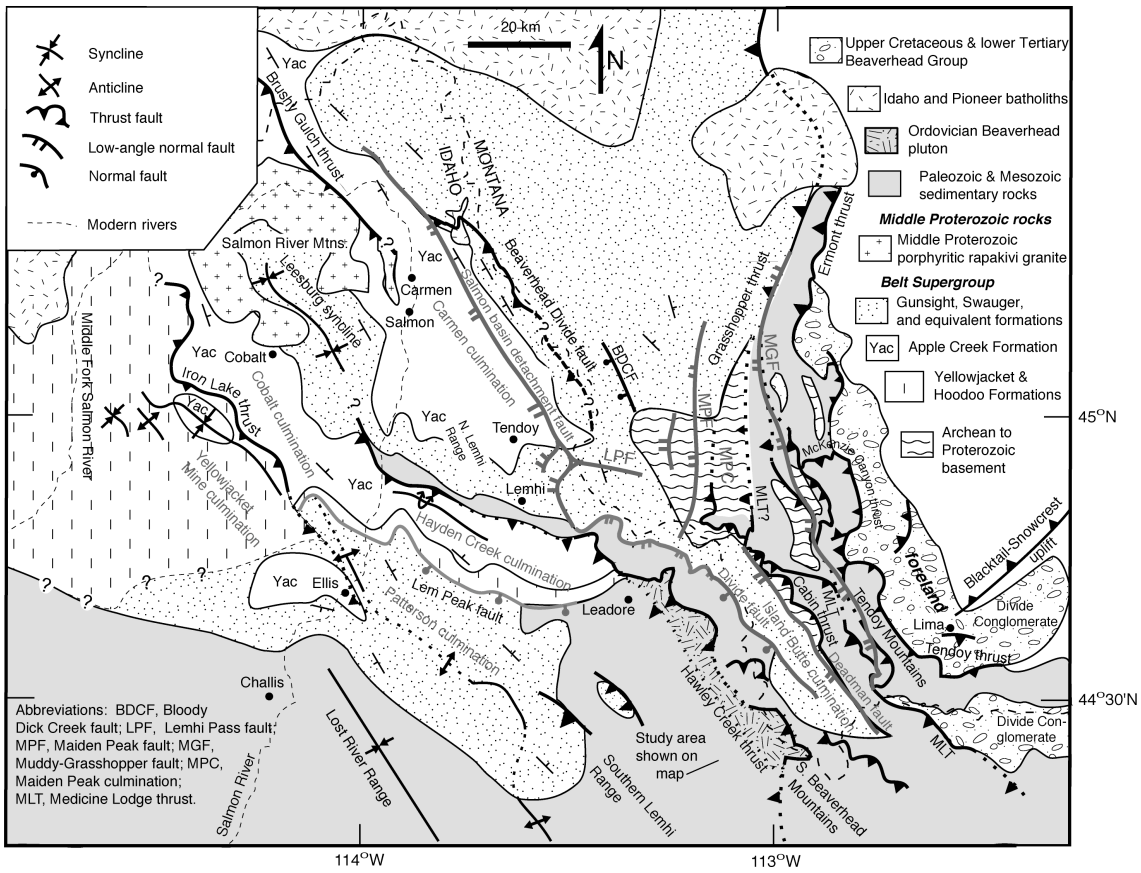

Figure 4. Middle Eocene subcrop map of the Idaho-Montana fold-and-thrust belt showing the locations of structural culminations and normal faults that eventually collapsed them. Map shows age of bedrock beneath middle Eocene Challis Group and was constructed by using principles outlined in Rodgers and Janecke (1992). Compiled from 80 sources in the data repository of Janecke et al. (2000). Normal faults of Eocene-Oligocene age are grayed. Notice the association between these large normal faults and structural culminations of the fold-and-thrust belt. Residual lateral density contrasts in the erosionally denuded structural culminations may explain the association of the culminations and detachment faults. Figure was modified from Janecke et al. (2001).

Late Cenozoic: Extension related to Basin-and-Range deformation is distributed over a broad area. Passage of the Yellowstone hot spot complicates the tectonics, and lateral flow of mid and lower crustal rock from the hotspot track may explain the anomalously high elevation of the region adjacent to the Eastern Snake River Plain (McQuarrie and Rodgers, 1998; Humphreys et al., 2001). Basin-and-Range extension produced the SW-dipping Beaverhead range-front fault south of the Salmon basin (Fig. 4). Few Basin-and-Range faults cut the Salmon basin.

GEOLOGY OF THE SALMON BASIN

Prior mapping in the basin by Anderson (1956, 1957, 1959, 1961), Ruppel et al. (1993) Tucker (1975), and sedimentologic analysis by Harrison (1985) showed that coarse marginal deposits surrounded a central core of

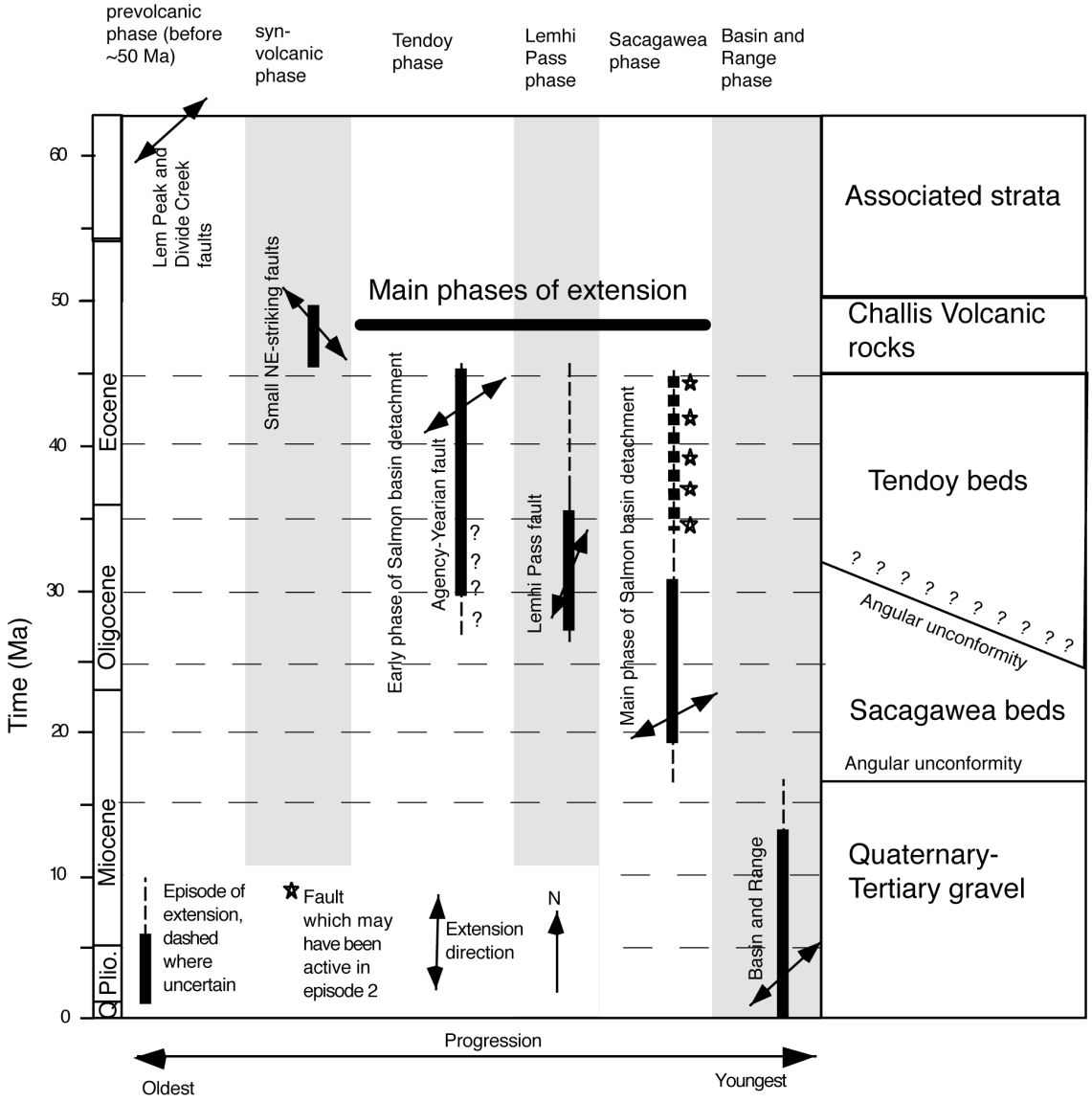

Figure 5. Sequence of extensional events in the SE part of the Salmon basin. The absolute ages of events and syn-rift deposits are poorly known but cross cutting relationships show that, during the main phases of extension, the Agency-Yearian fault formed first. It was probably the SE part of the Salmon basin detachment fault. Later, the Lemhi Pass fault offset and reoriented the Agency-Yearian fault and folded its northern part into the large SE-trending rollover anticline. The Salmon basin detachment fault was reestablished and developed a new trace during the Sacagawea phase. Minor synvolcanic extension and Basin-and-Range extension affected the SE part of the Salmon basin. Tysdal (1996a, 1996b; 2002), Tysdal and Moye (1996), and VanDenburg et al. (1998) document a pre-volcanic phase of extension that could date from Cretaceous time.

lacustrine deposits, and that high-angle normal faults defined the northeast and western margin of the triangular Salmon basin (Figs. 1, 3). Structural mapping

was reconnaissance in nature and lateral correlations of subunits within the basin fill were unknown or disputed (Anderson 1956, 1957, 1959, 1961; Ross, 1962, 1963). The Salmon basin lies immediately north of Beaverhead Valley, a large NE-tilted half graben above an active Basin-and-Range normal fault (e.g., Crone and Haller, 1991). The Salmon basin shares a common footwall with the Beaverhead Valley to the south (Fig. 3) but is clearly a different type of basin than the deep, active Beaverhead half graben because 1) its basin-bounding fault is no longer active (e.g., Crone and Haller, 1991; Blankenau, 1999); 2) the basin-fill deposits are uplifted and being dissected by tributaries of the Salmon River, whereas exposures of Cenozoic basin fill in the Beaverhead Valley are limited to uplifted fault blocks along the margin of the basin (Bond, 1978); 3) gravity data shows that the basement beneath the Salmon basin is close to the surface, unlike the deep and locally steep-sided Beaverhead basin (Bankey and Kleinkopf, 1988); and 4) the basin-bounding normal fault to the Salmon basin is a low-angle detachment fault with significant slip (Tucker and Birdseye, 1989; Janecke et al., 1998; Blankenau, 1999; Janecke et al., 2001), not a moderately dipping Basin-and-Range normal fault. The first study to note the possible detachment fault along the northeast margin of the Salmon basin also described mylonite in its footwall along Kenney Creek (Tucker, 1983; Tucker and Birdseye, 1989). Blankenau observed foliated cataclasite, not mylonite, in the footwall of the Salmon basin detachment fault, but confirmed the low-angle geometry of the basin-bounding normal fault (Blankenau, 1999; Janecke et al., 2001 and unpublished reconnaissance).

In order to begin to understand the structural and tectonic significance of the Eocene-Oligocene extensional province, Blankenau (1999) mapped a large area in the southeast part of the Salmon basin, in part to test our working hypothesis that the Salmon basin is a supradetachment basin, not a simple graben bounded by high-angle faults. Reports of low-angle normal faults (Tucker, 1983; Tucker and Birdseye, 1989) plus our discovery of possible large, map-scale extensional folds on aerial photographs motivated us to focus on the southeast portion of the Salmon basin.

Two sequences of sedimentary syn-rift deposits, separated by an angular unconformity, crop out in the SE part of the Salmon basin. The older Tendoy beds overlie the pre-rift to early-rift Challis Volcanic Group in slight angular unconformity, whereas the younger Sacagawea beds were deposited across older extensional structures that formed during and after deposition of the Tendoy beds (Blankenau, 1999). The Sacagawea beds are limited in their aerial distribution but may correlate to the northwest with more widely distributed deposits. The Tendoy beds formed in response to slip across the Agency-Yearian detachment fault (Blankenau, 1999), an older deactivated strand of the Salmon basin detachment fault. The Agency-Yearian fault was offset by a cross fault and then abandoned (Blankenau, 1999). The Sacagawea beds were deposited during slip on a new strand of the Salmon basin detachment.

Our division of subunits within the pre-rift volcanic rocks and syn-rift sedimentary rocks differs significantly from prior usage, particularly in the syn-rift deposit (e.g., compare Blankenau (1999) with Anderson (1956, 1957, 1959, 1961), Tucker (1975), Staatz (1979), and Harrison (1985)). We applied new local names to this stratigraphic succession, and like Harrison (1985), abandoned the nomenclature of Anderson due to its inconsistent application. It is not clear whether Blankenau's local stratigraphy of older Tendoy beds and younger Sacagawea beds will be useful elsewhere in the Salmon basin because the structural evolution of the southeast part of the Salmon basin is unusually complex (Blankenau, 1999). Reorientation and disruption of the ancestral Salmon basin detachment fault (=Agency-Yearian fault) by the Lemhi Pass cross-fault produced subbasins, angular unconformities and discrete, unconformity-bounded sequences of syn-rift sediment in the southeast part of the Salmon basin which may correlated with a single growth sequence away from the Lemhi Pass fault. Large fault-bend folds above the basin-bounding detachment fault may also be concentrated in the SE part of the Salmon basin.

Our understanding of the chronology of the Salmon basin is incomplete because the syn-rift deposits contain little datable volcanic material. The underlying Middle Eocene Challis Volcanic Group is now well dated between 49.51±0.14 and 45.95±0.12 (Janecke and Snee, 1993; M'Gonigle and Dalrymple, 1993 and 1996; VanDenburg et al., 1998; data of Blankenau, Janecke, and McIntosh reported in Blankenau, 1999) but Challis rocks merely provide a maximum age for the extensional phase that produced the Salmon supradetachment basin.

The age of the syn-rift deposits is based on a single crystal $^{40}Ar/^{39}Ar$ age determination on sanidine in an ashfall tuff (Axelrod, 1998). A date of 30.60±0.07 Ma was determined for crystals from a thin tuff within flora-bearing bentonite of the Snook quarry, near the mouth of Haynes Creek (Axelrod, 1998) (Fig. 4). Although it is most likely that the enclosing shale and mudstone succession is part of the Tendoy beds (e.g., Fig. 6), it is possible that the dated beds correlate with the younger, aerial less extensive Sacagawea beds. The correlation with the Sacagawea beds is not preferred because the dated beds are lacustrine whereas the Sacagawea beds are coarse fluvial and sediment gravity-flow deposits.

Unlike many Tertiary basins in the region (e.g., Fields et al., 1985; Nichols et al., 2001), the Salmon basin lacks vertebrate remains from which its age could be inferred. The lacustrine facies that dominate the center of the basin (Harrison, 1985) and marginal pebble to boulder conglomerate do not produce remains of land mammals. In addition, the Salmon basin had a more humid climate than many of the vertebrate-bearing basins in southwest Montana (Axelrod, 1998). Humid conditions favor preservation of floral remains over faunal remains (G. Retallack, oral. comm., 2002).

The poor age control in the syn-rift rocks in this supradetachment basin is particularly unfortunate because the basin fill has yielded several extensive floral collections (Wolfe and Wehr,

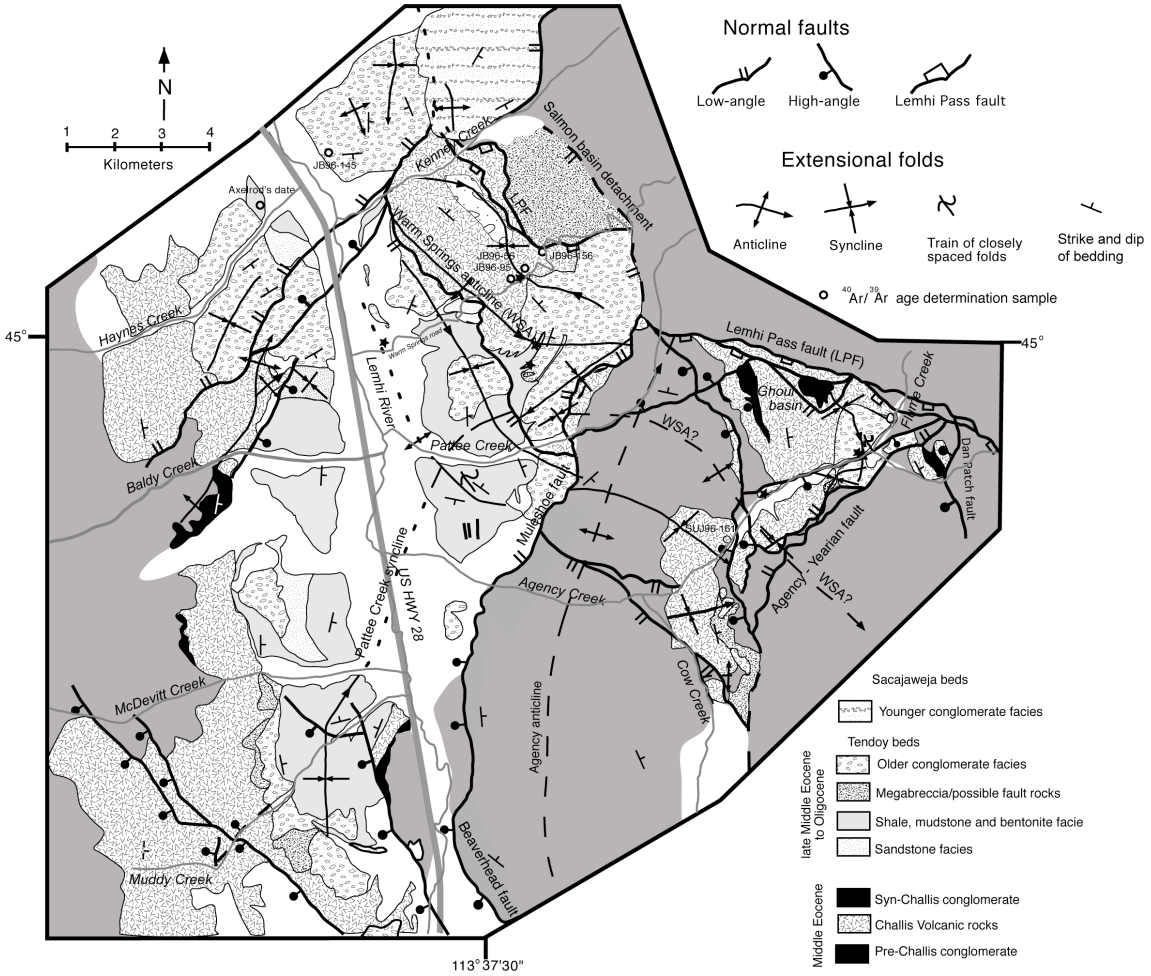

Figure 6. Simplified geologic map of the SE part of the Salmon supradetachment basin. Mapping by Blankenau and Janecke. The supradetachment basin is essentially an E to NE-tilted half graben in the hanging wall of the Agency-Yearian and Salmon basin faults. Extensional folds formed during multiple phases of extension, and some younger, superimposed normal faulting complicates the geometry of the basin. Intersecting early NNE-trending folds and younger NW-trending folds locally produce dome-and-basin structure and segmented the basin during sedimentation. Approximate locations of field trip stops are shown as stars.

1987; Axelrod, 1998), which provide clear pictures of the paleoecological conditions at the time of deposition and could constrain the paleoelevation of the region. The paleoelevations of the flora are debated, with Wolfe and Wehr (1987) originally suggesting that the Salmon flora grew in cooler conditions (and presumably at higher elevations) than the possible high-elevation Florissant flora of central Colorado, and Axelrod (1998) concluding that the elevation of his nearby Haynes Creek locality was about 1000 m. Axelrod's

estimate is several hundred meters below the present elevation and Wolf and Wehr's data imply high elevations above the present. Tectonic models of the Sevier thrust belt and its subsequent collapse depend on resolution of this debate, and on quantifying the post-contractional extension across the major normal faults in the region.

Little was known about the structural geology of the Salmon basin prior to our study. It has been clear for many years that the SW-dipping normal fault at the base of the Beaverhead Mountains (also called the Bitterroot Range) was a major structure but prior mapping showed a high-angle structure with a sinuous trace due to offsets on high-angle cross faults (e.g., Tucker, 1975; Ruppel et al., 1993). In addition, E-dipping normal faults were shown west of Salmon, along the entire western margin of the basin (Harrison, 1985; Ruppel et al., 1993). The curving southern boundary of the basin is a hanging-wall ramp of generally NE-dipping pre- and syn-rift rocks. Folding about N- to NE-trending extensional folds and normal faults complicates this hanging-wall ramp (Janecke et al., 1998) (Fig. 3b). Early work showed the Salmon basin as a full graben between northward converging normal faults.

At stop 1 we will view deposits along the western margin of the Salmon basin and show that this side of the basin is depositional with the pre-Tertiary bedrock north of Salmon, Idaho. At stop 2 we will observe the basin-bounding Salmon basin detachment fault along the northeast margin of the basin and see that it is a major low-angle normal fault with perhaps 5-10 km of slip. Subsequent stops within the southeast Salmon basin introduce the extensional folds that formed in association with Eocene-Oligocene normal faulting, facies patterns within the basin fill that resulted from intrabasinal deformation, and shoestring deposits within the Cretaceous (?) to Eocene Lemhi Pass paleovalley.

Kinematic classification of extensional folds

Extensional folds are common in the Salmon basin (Fig. 7). Such folds may be parallel (longitudinal), perpendicular (transverse) or oblique to the formative normal fault (Schlische, 1996; Janecke et al., 1998). The most common type of extensional folds, the well-known rollover monocline, is often the most conspicuous and largest type of extensional fold outside of metamorphic core complexes. Rollover monoclines form above listric normal faults (Xiao and Suppe, 1992). More subtle extensional folds develop when there is a displacement gradient along normal faults, when faults propagate up-dip or along strike, and whenever normal faults bend along strike or down dip. These processed produce displacement-gradient folds, fault-propagation folds and fault-bend folds respectively (Schlische, 1996; Janecke et al., 1998). There are several large rollover anticlines in the southeast Salmon basin that are sometimes flanked by parallel synclines. Fault-bend folding processes appear to have been prominent in the structural development of the southeast Salmon basin (Blankenau, 1999).

FIELD TRIP GUIDE:

The Salmon and Leadore 30' by 60' topographic quadrangles are helpful for navigation on the many small roads in

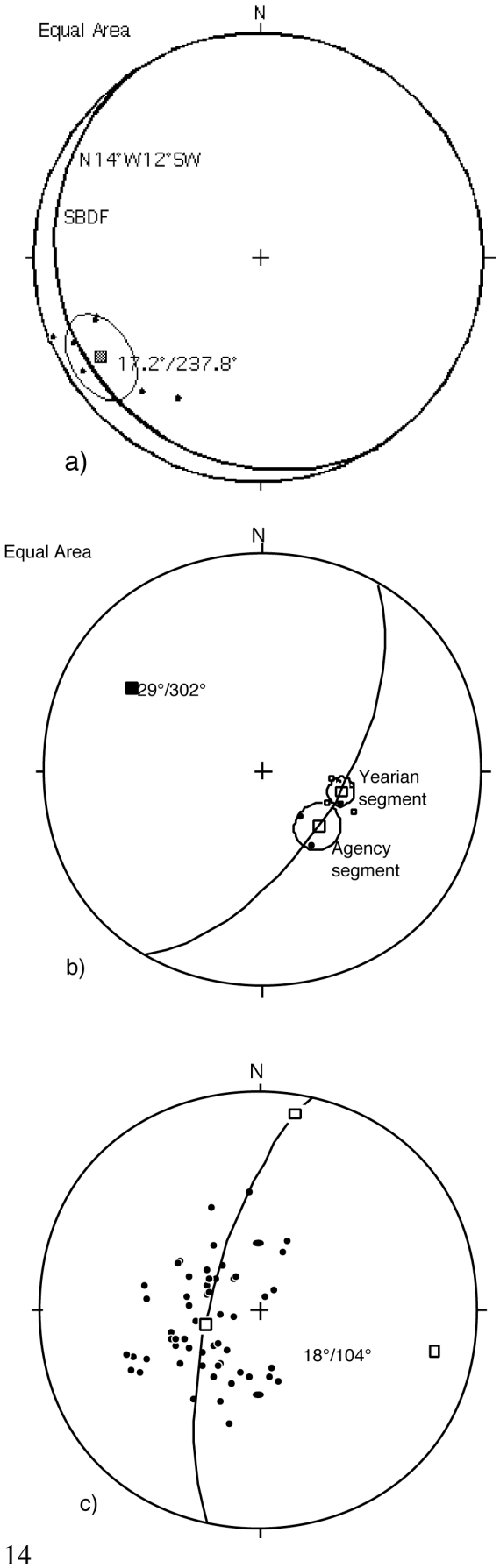

Figure 7. Stereograms of structural data from the Salmon basin. a) Orientation of the Salmon basin detachment fault along Kenney Creek, with WSW plunging slickenlines. Note the low dip of the fault. b) Stereograms of poles of fault surfaces that show that the intersection of the NW-dipping Agency segment of the AYF with the W-dipping Yearian segment defines a NW-trending fold that is along trend of the WSA. The WSA has an identical trend (Fig. 7d). c) Poles to bedding of Mesoproterozoic rocks in the core of the Agency anticline from Staatz (1979). The fold axes define an ESE-trending fold that we interpret as a southeast continuation of the WSA. The NNE trending agency anticline is not evidence in these data. d) Nine stereograms of structural data from extensional folds in the Salmon basin. The great circle and poles of the normal fault that produced the fold is shown for reference. Abbreviations: LPF = Lemhi Pass fault, AYF = Agency-Yearian fault.

this area. Stops 3 to 8 are within the area studied by Blankenau (1999).

Stop 1 BLM campground along the Salmon River

After crossing the Salmon River, drive north on US 93 from the center of Salmon. Follow the signs on US 93 to the fairgrounds (approximately 3.75 miles north of the river crossing). Turn left toward the fairgrounds for about 0.5 miles but turn north onto the road at the base of the hills from US 93 to the west. Drive north along this road for about 1.5 miles and watch for exposures of

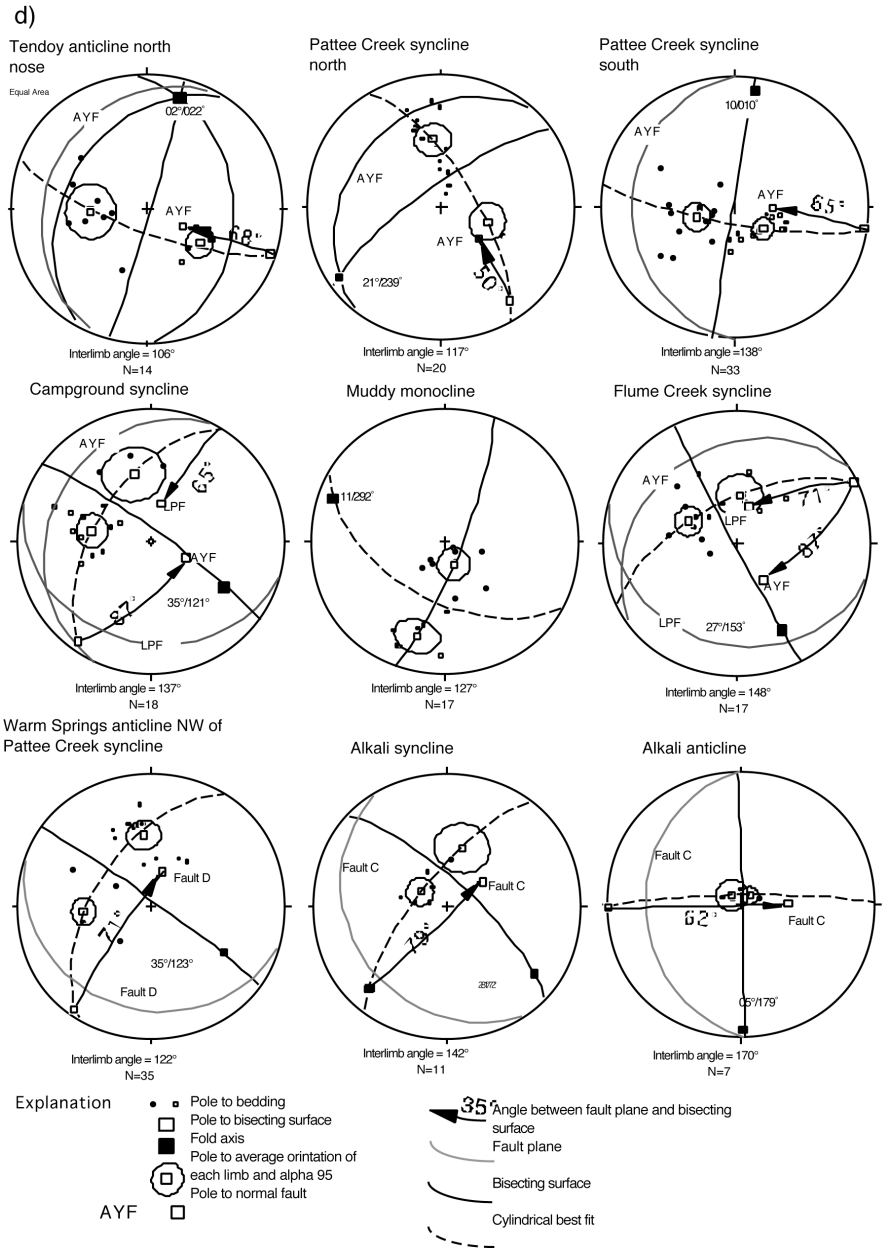

conglomerate that are in depositional contact with the underlying Belt rocks. Keep going until a BLM campground appears on the right and cliffs of boulder conglomerate are on the left. Park and walk over to examine these exposures.

Structurally, the Salmon basin is as ENE-tilted half graben, not a full graben. Volcanic rocks of the northern Lemhi Range generally dip ENE toward the Salmon basin detachment fault along the SW front of the Beaverhead Mountains. The geometry of the basin is more complex, however, due to folding and cross-faulting (Fig. 3).

The western margin of the Salmon basin exposes the contact between middle Proterozoic Belt rocks and the Eocene-

Miocene (?) basin-fill deposits. Middle Eocene Challis rocks are lacking along this depositional contact but are present 15 km to the south and about 10 km to the north. The absence of Challis rocks in this intervening area (e.g., Ruppel et al., 1993) is likely due to non-deposition near the east margin of the Challis volcanic field and/or erosion within a Cretaceous (?) to Eocene SE-draining paleovalley (Janecke et al., 2000). The lens-shaped outcrop pattern in the conglomerates to our west is consistent with deposition in an east-sloping paleovalley. Subsequent eastward tilt produced an oblique cross section of the paleovalley fill.

Most prior maps interpret an E-dipping normal fault along the basin margin near stop 1 (Harrison, 1985; Ruppel et al., 1993) but these boulder conglomerates are clearly in depositional contact with Proterozoic bedrock to the west. Any E-dipping normal fault must lie within the basin-fill rather than bound the basin-fill on the west. The boulder conglomerate dips gently east, parallel to the gently east-dipping depositional contact, and it contains numerous clasts of a distinctive porphyritic granite of Mesoproterozoic age which is exposed a few kilometers to the west (Evans and Zartman, 1990; Doughty and Chamberlain, 1996). The main body of the granite lies even farther west.

The Mesoproterozoic rapakivi granite is a point source of distinctive clasts that were carried SE in Eocene rivers for at least 75 km into western Montana (Janecke et al., 2000) (Fig. 4). We stopped here to observe this distinctive lithology and to note the depositional contact with the underlying bedrock. The contact is not visible from this stop but is apparent from other roads in this area.

Retrace route back to Salmon. Drive through Salmon on US 93 and continue past traffic light at intersection of Idaho 28 and US 93 . Drive southeast for about 8 miles on Idaho 28 past the traffic light to the hamlet of Baker. Turn east and drive 0.6 miles on spur road and for access to the frontage road on the east side of the Lemhi River. At T intersection turn north (left) for 0.1 miles. Turn east (right) onto dirt road into Wimpey Creek drainage. After 1.9 miles pull off the Wimpey Creek road right before the road begins to descend down from the high terrace level into the drainage.

Stop 2 in Wimpey Creek

This area is north of the our 1:24,000 scale mapping in the southeast part of the Salmon basin but we stop here to view the Salmon basin detachment fault in an more accessible location. Detailed mapping of the faults and its syn-rift deposits is needed here to build on the 1:62,500 scale mapping of Tucker (1975).

View to the NE of the low-angle detachment fault with reddish syn-rift deposits in its hanging wall. The road cuts and surfaces north of the road expose conglomerate that contains rounded clasts of the Mesoproterozoic Apple Creek Formation. Note that the Challis volcanic rocks are not present in the source terrane at this time, despite their great thickness on the west side of the basin.

Notice how fine grained the basin fill is near the basin bounding normal fault. Mud and sand are very prominent here

within 1-3 km of the Salmon basin detachment fault. This grain size is inconsistent with the predictions of a facies model by Friedman and Burbank (1995) for supradetachment basins. Coarse conglomerate and rock avalanche deposits should extend for 5-10 km into the basin according to the Friedman and Burbank model (1995).

There appears to be a low cut-off angle between the basin fill and the low-angle fault surface that you see in the distance. If confirmed, this relationship demonstrates that the Salmon basin detachment fault was active at low angles. (The variable, steeper orientation of Tertiary basin fill deposits in the pointy hill near us are due to deformation along a steep NE-striking fault that parallels Wimpey Creek (Tucker, 1975), and does not provide insights into the original dip of the detachment fault.)

Turn around and drive back down Wimpey Creek toward the main highway (Idaho 28). Notice that the dark lava flows on the west side of the Lemhi Valley dip toward us and are overlain by white tuffs of the youngest phase of Middle Eocene Challis volcanism. After returning to the main road (Idaho 28) drive southeast for 6 miles. Turn left (east) onto spur to access frontage road. At the T intersection drive south for 2 miles to Warm Springs road on your left. Turn east (left) and drive on Warm Springs road for 0.7 miles to the Lewis and Clark informational kiosk on your left. A short walk to the south side of the road, onto a small hill, provides a better viewpoint.

Stop 3 Lewis and Clark informational kiosk along Warm Springs road.

At this stop we will become oriented to the southeast part of the Salmon supradetachment basin. This part of the basin appears to be the particularly complex, both structurally and stratigraphically. Much of the rest of the basin contains lacustrine deposits in its center and marginal sandstones and conglomerates (Harrison, 1985). We drove past large areas of banded lacustrine rocks on our way here. The basin-fill north of here is deformed by gentle folds and smaller normal faults (e.g., Tucker, 1975) but the intensity of deformation (based on the tilt of the beds) appears to be greatest in the southeast part of the basin.

The rocks visible from at stop 3 can usually be identified based on their color and resistance to erosion (Fig. 6). Dark resistant looking rocks are part of the Mesoproterozoic Belt Supergroup. The Apple Creek and Gunsight formations both crop out in this area according to Lund et al. (2003). The Belt rocks can be confused with dark exposures of Eocene Challis lava flows. These are present both on the west side of the basin and in the core of the very large Warm Springs anticline, northeast of us. These dark lavas overlie and are overlain by lighter ash flow tuffs of the Challis Group. Above the Challis volcanics are Eocene to Miocene (?) conglomerate, sandstone, mudstone, shale, and local megabreccia deposits of the syn-rift Tendoy beds. Volcanic–clast conglomerates underlie dark rolling hills visible from this stop. Lake beds may be light in color, and can be confused with tuffaceous intervals in the older Challis volcanic from a distance. Yellow units are typically quartzose sandstones of the

Tendoy beds with interbeds of conglomerate.

East of here the map pattern and strike and dip data define a major SE-plunging anticline (Janecke et al., 1998; Blankenau, 1999) (Fig. 6). The southwest margin of this Warm Springs anticline was later cut by a major SW-dipping normal fault. We are standing on mud to conglomerate of the Tendoy beds in the hanging wall of that younger fault. Exposures are somewhat limited in the hanging wall of the SW-dipping normal fault but it is clear from Blankenau's mapping and air photo work that a SE-trending syncline parallels the normal fault and lies 0.2 to 0.7 km SW of its surface trace. Synclines often occupy the hanging walls of normal faults in this area, and are a characteristic structural motif of extending regions (Blankenau, 1999; Janecke et al., 1998).

Continue driving up Warm Springs road for another 1.7 miles to exposures of ashflow tuffs on your left.

Stop 4 Folded ashflow tuffs of the Challis Volcanic field along Warm Springs road

Examine the youngest units of the Challis Volcanic Group in this area. The quartz and sanidine-bearing ashflow tuff is the youngest laterally continuous unit in this area (Staatz, 1979; Blankenau, 1999). It is about 46 Ma based on two age determinations (Table 2). The underlying Tuff of Curtis Ranch is also a rhyolite but is 1.5 Ma older. It has an age of 47.58±0.14 Ma on sanidine (Table 2). Both tuffs are white but the abundant biotite in the Tuff of Curtis Ranch, with prominent pumice lapilli in some zones, distinguish it from the quartz and sanidine bearing ashflow tuff.

These two ashflow tuffs are widely distributed across the region (M'Gonigle and Dalrymple, 1993, 1996; Blankenau, 1999). This shows that topographic barriers that controlled the distribution of ashflow tuffs at the base of the Challis succession had filled and been buried by volcanic rock by 47-46 Ma (Janecke et al., 2000).

Find a turn around and drive back downhill along the Warm Springs road until the Alkali Flats road on your left. Turn south onto Alkali Flats road and drive 1.7 miles until you see some outcrops of conglomerate on your left. Pull over for stop 5.

Stop 5 Tendoy beds along the Alkali Flats road

Examine outcrop of angular-clast conglomerate of the Tendoy beds and float of intervening tuffaceous shale. The conglomerate here is very angular to sub-angular, matrix to clast supported, with a tan tuffaceous matrix. Clasts range from pebbles to cobbles with a maximum grain size of 20 cm. The conglomerate is typically dominated by quartzite clasts, except within ~ 100 m of its base where it contains mostly volcanic clasts. It ranges from being well to poorly cemented. Where the conglomerate is well cemented it forms resistant fins. Interbeds of lithic arenites are also present. The conglomerate facies interfingers with the shale unit, and sandstone beds are rare (Blankenau, 1999).

Between the ribs of conglomerate are white to tan very finely laminated to massive, non-calcareous, tuffaceous

TABLE 2. NEW AGE DETERMINATIONS FROM THE SOUTHEAST SALMON BASIN (data of Blankenau, Janecke, and McIntosh in Blankenau, 1999)

Sample number	Rock type	Location (latitude / longitude)	Method	Age Ma	Comments
JB96-156	lava flow or shallow intrusive	Sect. 34; R24E; T20N (45°1'17" / 113°35'51")	$^{40}Ar/^{39}Ar$ step-heating of a groundmass concentrate	36.85± 0.16	highly disturbed unreliable
JB96-95	tuff of Curtis Ranch (Tcr)	Sect. 34; R24E; T20N (45°0'21" / 113°36'25")	$^{40}Ar/^{39}$ single sanidine crystals	47.58± 0.14	excellent age determination
JB96-56	quartz sanidine tuff 2 (Tqs2)	Sect. 34; R24E; T20N (45°0'26" / 113°39'32")	$^{40}Ar/^{39}$ single sanidine crystals	46.13± 0.19	reliable; same unit as SUJ96-161
JB96-145	intrusion (Ti) into Tcg3	Sect. 30; R24E; T20N (45°1'58" / 113°39'32")	$^{40}Ar/^{39}$ step-heating of a groundmass concentrate	37.08± 0.21	Unreliable, plug intrudes Tcg3; highly disturbed spectrum.
SUJ96-161	quartz sanidine tuff 2 (Tqs2)	Sect. 19; R25E; T19N (44°57'33" / 113°32'30")	$^{40}Ar/^{39}$ single sanidine crystals	45.95± 0.12	reliable; same unit as JB96-56
SUJ96-131	Densely welded rhyolite tuff*	Sect. 19; R23; T20N (45°2'35" / 113°47'24")	$^{40}Ar/^{39}$ single sanidine crystals	49.51± 0.14	in Withington Creek caldera; excellent age determination

Notes: Age spectrum graphs of the age determinations are shown in Appendix A.
• = Ashflow tuff with lithics of Apple Creek Formation which may correlate with the quartzite-bearing ashflow tuff (Tqt).

shales, mudstones and bentonites. The shale unit is widely distributed throughout the center of the basin, and is well exposed along gullies and stream cuts. Excellent outcrops occur west of the Lemhi River along Muddy, tributaries of McDevitt, Baldy, and at the mouth of Haynes Creeks, and east of the Lemhi River along Agency, Pattee, and Kenney Creeks (Fig. 6). This unit represents a lake that formed after Challis volcanism (Blankenau, 1999).

The association of angular, locally derived conglomerate, or sedimentary breccia, with lacustrine shale shows that coarse alluvial fans prograded directly out into the Pattee Creek lake. Mountain fronts were steep and supplied the coarse quartzose sediment (Fig. 2). Lake levels fluctuated many times and produced a

thick interval of lateral interfingering between lake bed and alluvial fan deposits (Fig. 6).

Return to vehicle and continue driving southeast for another 0.1 miles to a dirt track on your right. Follow it for 0.2 miles and park. Walk east and down the slope.

Stop 6 Breccia south of Alkali Flats road

Examine a megabreccia interbedded with lacustrine deposits of the Paleogene Tendoy beds. The breccia overlies hundreds of meters of Tendoy beds but was derived from the underlying Tuff of Curtis Ranch. A source in the hanging wall of the basin is likely because the composition of the associated quartzite-clast conglomerates, which were derived from bedrock to the north or east, shows that that area had already been stripped of its volcanic cover by this time (stop 5).

The megabreccia is interpreted as a rock avalanche deposit that was emplaced into the basin during extension. The presence of the megabreccia indicated considerable tectonic unrest and topographic relief along the margins of the basin during deposition. Rock avalanche deposits are most common within the basal syn-rift sedimentary rocks on the hanging wall side of the basin, but they occupy other structural and stratigraphic positions as well (Blankenau, 1999) (Fig. 6).

Mapping of the syn-rift deposits southeast of here shows the presence of a very laterally continuous syncline. This Pattee Creek syncline folds the Tendoy beds and the underlying volcanic and metasedimentary rocks. The Tendoy beds preserved on the northwest limb of the Pattee Creek north syncline are about 1400 m thick whereas those on the southeast limb are only about 400 m thick (Blankenau, 1999). These relationships indicate growth of the Pattee Creek syncline and Agency anticline during deposition of the Tendoy beds. In addition, the thickness patterns show that the anticlinal hinge migrated northwestward over time.

Several data sets indicate that the Pattee Creek syncline and Agency anticline are fault-bend folds above the Agency-Yearian fault. The Pattee Creek syncline parallels the Tendoy anticline for its entire length of 11.8 km (Fig. 6). The northern segment of the syncline plunges 21° toward 239°, and has an interlimb angle of 117°. The angle between the strike of the adjacent part of the Agency-Yearian fault and the trend of the Pattee Creek south syncline fold axis is 22°, and the fold and fault have a 18° angle between them in the northern portion.

Physical models of fault-bend extensional folds by McClay (1989) match the fault and fold geometries and syntectonic sedimentation patterns around the Agency-Yearian fault, Agency anticline, and Pattee Creek syncline. Because the model closely matches the field observations, the Agency anticline and Pattee Creek syncline are interpreted as forming above a longitudinal ramp and flat in the underlying Agency-Yearian fault. The Agency anticline is interpreted as a rollover fold above the listric east part of the Agency-Yearian fault whereas the Pattee Creek syncline is interpreted as forming above a deeper ramp in the fault. This interpretation is consistent with the thickness variation in the syntectonic sedimentary rocks preserved

in the Pattee Creek north syncline and the change in the character of the conglomerates of the basal Tendoy beds on the two flanks of the Agency anticline (see below). Younger sets of normal faults have truncated the west flank of the Agency anticline (Fig. 6).

Retrace your steps to the frontage road and turn south. Drive about 3 miles south on the frontage road to the turn up toward Lemhi Pass. Turn east (left) onto the Agency Creek-Lemhi Pass road. Drive 6.6 miles through the core of the Agency anticline. Blankenau (1999) called this the Tendoy anticline but we use the new Agency name here to avoid confusion with structures in the Tendoy Mountains of southwest Montana. Pull off and park opposite steep slopes of pinkish ashflow tuff.

Stop 7 Quartzite bearing ashflow tuff in the Lemhi Pass paleovalley

Examine a diagnostic tuff of the Lemhi Pass paleovalley. The quartzite-bearing ashflow tuff is white, pinkish red, white gray, or pink gray, and contains abundant black quartzite clasts, lesser amounts of smoky quartz, sanidine, and plagioclase in a white ash matrix (Staatz, 1979; Blankenau, 1999). Typical quartzite lithics resemble the Apple Creek and Yellowjacket formations, and are dark gray to black, angular, micaceous, and 2-4 cm across, but are locally up to 20 cm across. The quartzite-bearing ashflow tuff is typically poorly welded, but may be densely welded. It has a maximum thickness of 430 m.

The spatial distribution of the quartzite-bearing ashflow tuff indicates that it was confined to an E-SE-trending paleovalley (Fig. 4). The quartzite-bearing ashflow tuff pinches out to the south and is cut to the north by the Lemhi Pass fault. An $^{40}Ar/^{39}Ar$ age determination on single sanidine crystals yielded a mean age of 48.64 ± 0.33 Ma for the quartzite-bearing ashflow tuff near Lemhi Pass (M'Gonigle and Dalrymple 1993, 1996; Janecke et al., 2000).

A caldera in the northern Lemhi Range (Ruppel et al., 1993; Janecke et al., 2000) was probably the source for this tuff. The distinctive quartzite lithics in this unit support a source caldera in the northern Lemhi Range where the widely exposed Yellowjacket/Apple Creek Formation (Ruppel et al., 1993) could have provided the black lithics (note that the new map of Evans and Green (2003) shows Gunsight Formation in this area). An $^{40}Ar/^{39}Ar$ age obtained from a quartzite-bearing ashflow tuff in the caldera along Withington Creek yielded an age of 49.51±0.14 Ma (sample SUJ96-131, Table 2). This age is somewhat older than other dates obtained from the quartzite-bearing ashflow tuff by M'Gonigle and Dalrymple (1996) but indicates that both ashes formed during initial Challis volcanism.

The quartzite-bearing ashflow tuff has been identified in many localities and defines a shoestring deposit (Janecke et al., 2000) (Fig. 2). The most distant occurrence known to our research group is in the northern Muddy Creek basin, in the northern Tendoy Mountains (Janecke et al, 1999). That location is ~50 km from here. Clasts of the 1370 Ma rapakivi granite do not occur as far downstream as the tuff, but have been identified in the upper Horse Prairie

basin of western Montana. Altogether these data indicate that a huge river system flowed ESE through this area, had headwaters northwest of Salmon, Idaho, and continued southeast into the Tendoy Mountains of southwest Montana.

Continue driving northeast along Agency Creek toward Lemhi Pass for another 1.5 miles. Examine exposures of the conglomerates in the Tendoy beds on the north side of the road. The road is narrow and windy, so please watch for traffic.

Stop 8 Conglomerates of the Flume Creek subbasin

We are in the Flume Creek subbasin of the Salmon basin, east of the Agency anticline (Blankenau, 1999) (Fig. 6). We have been driving generally upsection from the Belt rocks, up through the Eocene volcanic rocks until here, where we are viewing basal units of the basin fill. Roadcuts expose well-rounded conglomerate and gravel of the basin fill deposits. These pebble to cobble conglomerates are the basal units of the syn-rift Tendoy beds, and contain a significant fraction of volcanic clasts in addition to much material derived from the surrounding Proterozoic Belt rocks. This exposure is typical of the ~500 m thick exposure conglomerate within a structural basin produced by two intersecting synclines. The NE-trending syncline roughly parallels the Agency-Yearian normal fault, whereas the more prominent NW-trending Flume Creek syncline has an uncertain origin. The NE-trending fold was probably produced by fault-bend or fault-propagation processes.

Notice that this conglomerate contrasts significantly with the angular clasts conglomerate that we observed in the Pattee Creek subbasin of the Salmon basin (stop 5). There are no interbedded mudstones or shales here, nor is there any indication of sediment-gravity flow processes. Volcanic-clast conglomerates in the Pattee Creek subbasin on the other side of the Agency anticline are usually matrix-supported debris flow deposits. We tentatively interpret the well-rounded and relatively sorted conglomerates in the Flume creek subbasin as deposits of a braided stream (Fig. 2). The source of sediment here in the Flume Creek subbasin is also different from that in the Pattee Creek subbasin (Blankenau, 1999).

The contrasting facies and provenance of coeval synrift deposits adjacent to the Agency anticline are consistent with the paleogeographic model in Figure 2. This basin was segmented by extensional folds.

Return to the vehicles and drive east to Lemhi Pass.

Stop 9 Lemhi Pass

Pull into the Sacagawea campground east of the pass and park in the large pull out shortly before the small campground area.

Examine another segment of the Lemhi Pass paleovalley and discuss the Lemhi Pass fault. At this stop we are at the continental divide between the Salmon River drainage on the west and the headwaters of the Missouri River on the east. These flow to the Pacific and Gulf of Mexico, especially. Both drainage systems are incising into older Cenozoic basin-fill deposits, exposing them for

study. This incision may be partly driven by lower crustal processes adjacent to the Yellowstone hotspot (McQuarrie and Rodgers, 1998; Humphreys et al., 2001).

We will examine quartzite-bearing ashflow tuff within the Lemhi Pass paleovalley and conglomerate of the river system that occupied the paleovalley both before and after the quartzite-bearing ashflow tuff rumbled eastward through this area.

Lemhi Pass fault and Summary

This stop is a good place to discuss the enigmatic Lemhi Pass fault, which was named for the pass near us. This fault was mapped by Staatz (1979) and shown to dip steeply SSW. The fault has about 7.5 km of right separation and likely has considerable dip slip as well (VanDenburg et al., 1998; Blankenau, 1999). VanDenburg and Blankenau mapped the southeastern and northwestern ends of this fault, respectively but the middle portion of the fault, near the pass has not been remapped by our group. In the lower elevations the Lemhi Pass fault has a low dip and contains the Warm Springs anticline in its hanging wall (Fig. 6). The Warm Springs anticline appears to extend SE across the Agency anticline, fold the Agency-Yearian strand of the Salmon basin detachment system, and continue into the footwall of that fault (Blankenau, 1999) (Figs. 6 and7). We interpret the Warm Springs anticline as a rollover anticline above a listric Lemhi Pass fault. We therefore expect that the Lemhi Pass fault will be steeper in the pass area than at lower elevations. This interpretation is consistent with the steep dips described by Staatz (1979) and the lower dips that we observe at lower elevations in Idaho and Montana (22-24°; VanDenburg et al., 1998; Blankenau, 1999).

The Lemhi Pass fault cuts the northeast end of the Agency-Yearian fault, defines the abrupt northern margin of the Flume Creek subbasin, and deforms structures and basins forming during the Tendoy phase of deformation (Blankenau, 1999)(Fig. 5, 6 and 7). The Lemhi Pass fault produced much of the structural complexity of the southeast part of the Salmon basin.

The origin of the Lemhi Pass fault is unclear. This fault is a major cross structure, at an angle to the dominant structural grain of the region, and it interrupts a relatively stable history of ENE-WSW extension (Fig. 5) (e.g., VanDenburg et al., 1998; Blankenau, 1999). The dominant extension direction in this area can be understood as "undoing" the shortening of the older Sevier fold-and-thrust belt (e.g., Janecke et al., 2001). The large normal faults parallel the thrusts in this region and reactivate them in places (e.g., Janecke, 1996). Thus gravitational collapse or reactivations of weak preexisting structural elements likely explains the major phases of extension along the Muddy-Grasshopper, Salmon basin, Maiden Peak, and Agency-Yearian detachment faults. Such a model cannot account for slip on the Lemhi Pass fault, however, because this fault is at a high angle to the overall structural grain of the region (Figs. 3, 4).

Whatever its origin, there is no doubt that the Lemhi Pass fault had a profound effect on the structural and basin evolution in both adjacent supradetachment basins. In the Salmon

basin, the Lemhi Pass fault so deformed the basin-bounding fault (the Agency-Yearian strand of Salmon basin detachment system) that a new strand of the Salmon basin detachment fault was initiated. This new strand cut across the original footwall and hanging wall of the older strand (Fig. 6). In the Horse Prairie basin, east of us, the Lemhi Pass fault deformed the early syn-rift deposits (Bear Creek beds) but was overlapped by younger syn-rift rocks of the Everson Creek beds (VanDenburg, 1997; VanDenburg et al., 1998). In the Horse Prairie basin, like in the Salmon basin, angular unconformities in the syn-rift deposits are most prominent near the Lemhi Pass fault. In the Grasshopper basin to the north, deformation, uplift, and erosion of early syn-rift deposits, and incorporation of older syn-rift sediment into younger syn-rift deposits is most prominent near major SE-plunging extensional folds that are coeval with, and subparallel to, the Lemhi Pass fault (Kickham, 2002; Matoush, 2002; Janecke unpublished data).

Cross faulting on the Lemhi Pass fault and related structures did not end the period of detachment faulting in the Salmon basin and adjacent areas, but it interrupted and reoriented the original systems of structures so much that new faults had to break across the deformed rocks masses, allowing WSW-ENE extension to continue. Listric low-angle normal faults accommodated this extension and produced the supradetachment basins of eastern-central Idaho and western Montana.

Return to vehicles and retrace route to Salmon. End of trip.

Acknowledgements:

Funding was provided by the National Science Foundation. Acknowledgment is also made to the donors of the American Chemical Society Petroleum Research Fund for partial support of this research. We thank landowners for access to their land, the BLM for use of color aerial photographs, and Daniel Axelrod for data in advance of publication. Stereograms were produced during Allmendinger's Stereonet program. Stephanie Carney provided editorial and graphic assistance and Jim Evans reviewed the manuscript.

REFERENCES CITED

Anderson, A.L., 1956, Geology and mineral resources of the Salmon quadrangle, Lemhi County, Idaho: Idaho Bureau of Mines and Geology Pamphlet 106, 102 p.

Anderson, A.L., 1957, Geology and mineral resources of the Baker Quadrangle, Lemhi County, Idaho: Idaho Bureau of Mines and Geology Pamphlet 112, 71 p.

Anderson, A.L., 1959, Geology and mineral resources of the North Fork Quadrangle, Lemhi County, Idaho: Idaho Bureau of Mines and Geology Pamphlet 118, 92 p.

Anderson, A.L., 1961, Geology and mineral resources of the Lemhi Quadrangle, Lemhi County, Idaho: Idaho Bureau of Mines and Geology Pamphlet 118, 92 p.

Armstrong, R.L., 1975, The geochronometry of Idaho: Isochron West, v. 14, p. 1-50.

Axelrod, D.I., 1998, The Oligocene Haynes Creek flora of eastern

Idaho: University of California Publications in Geological Sciences, v. 143, 99 p.

Axelrod, D.L., 1968, Tertiary floras and topographic history of the Snake River basin, Idaho: Geological Society of America Bulletin, v. 79, p. 713-734.

Bankey, V., and Kleinkopf, M.D., 1988, Boulder gravity anomaly map and four derivative maps of Idaho: U.S. Geological Survey Geophysical Investigations Map GP-978, scale 1:1,000,000.

Blankenau, J.J., 1999, Cenozoic structure and stratigraphy of the southeast Salmon basin, east central Idaho [M.S. thesis]: Utah State University, 142 p.

Bond, J.G., 1978, Geologic map of Idaho: Idaho Bureau of Mines and Geology, scale 1:500,000.

Burchfiel, B.C., Cowen, D.S., and Davis, G.A., 1992, Tectonic overview of the Cordilleran orogen, *in* western United States, in Burchfiel, B.C., Zoback, M.L., and Lipman, P.W., eds., The Geology of North America, v. G-3, The Cordilleran Orogen: Conterminous U.S., Geological Society of America, Bolder CO, p. 407-480.

Crone, A.J., and Haller, K.M., 1991, Segmentation and coseismic behavior of Basin and Range normal faults: Examples from east-central Idaho and southwestern Montana, U.S.A.: Journal of Structural Geology, v. 13, p.151-164.

Doughty, P.T., and Chamberlain, K.R., 1996, Salmon River arch revisited: new evidence for 1370 Ma rifting near the end of deposition in the Middle Proterozoic Belt basin: Canadian Journal of Earth Science, v. 33, p.1037-1052.

Evans, K.V., Aleinikoff, J.N., Obradovich, J.D., and Fanning, C.M., 2000, SHRIMP U-Pb geochronology of volcanic rocks, Belt Supergroup, western Montana; evidence for rapid deposition of sedimentary strata: Canadian Journal of Earth Sciences, v. 37, p. 1287-1300.

Evans, K.V., and Green, G.N., 2003, Geologic map of the Salmon National Forest and vicinity, east-central Idaho: U.S. Geological Survey Miscellaneous Investigations Map I-2765.

Evans, K.V., and Zartman, R.E., 1990, U-Th-Pb and Rb-Sr geochronology of Middle Proterozoic granite and augen gneiss, Salmon River Mountains, east-central Idaho: Geological Society of America Bulletin, v. 102, p. 63-73.

Fields, R.W., Rasmussen, D.L., Tabrum, A..R, and Nichols, R., 1985, Cenozoic rocks of the intermontane basins of western Montana and eastern Idaho; a summary, *in* Flores, R.M., and Kaplan, S.S., eds., Cenozoic paleogeography of the west-central United States: Rocky Mountain Section of the Society of Economic Paleontologists and Mineralogists, Denver, CO, p. 9-36.

Foster, D.A., Mueller, P.A., Heatherington, A.L., Vogl, J., Meert, J., Lewis, R., and Wooden, J.L., 2002, Configuration of the 2.0 –1.6 Ga accretionary margin NW of the Wyoming province:

Implications for Proterozoic continental reconstructions: Geological Society of America Abstracts with Programs, v. 34, p. 559.

Foster, D.A., and Fanning, C.M, 1997, Geochronology of the northern Idaho Batholith and the Bitterroot metamorphic core complex; magmatism preceding and contemporaneous with extension: Geological Society of America Bulletin, v.109, p. 379-394.

Friedmann, S.J., and Burbank, D.W., 1995, Rift basins and supradetachment basins: Intracontinental extensional end-members: Basin Research, v. 7, p. 109-127.

Hargraves, R.B., Cullicott, C.E., Deffeyes, K.S., Hougen, S., Christiansen, P.P., and Fiske, P. S., 1990, Shatter cones and shocked rocks in southwestern Montana: The Beaverhead impact structure: Geology, v. 18, p. 832-834.

Harrison, S., 1985, Sedimentology of Tertiary rocks near Salmon Idaho: [Ph.D. dissertation]: University of Montana, 175 p.

Humphreys, E.D., Dueker-Kenneth, G., Schutt, D.L., Smith, R.B, 2001, Beneath Yellowstone; evaluating plume and nonplume models using teleseismic images of the upper mantle: GSA Today, v. 10, p. 1-7.

Janecke, S.U., 1992, Kinematics and timing of three superposed extensional systems, east-central Idaho: Evidence for an Eocene tectonic transition: Tectonics, v. 11, p.1121-1138.

Janecke, S.U., 1994, Sedimentation and paleogeography of an Eocene to Oligocene rift zone, Idaho and Montana: Geological Society of America Bulletin, v. 106, p. 1083-1095.

Janecke, S.U., 1995, Eocene to Oligocene half grabens of east-central Idaho: Structure, stratigraphy, age, and tectonic: Northwest Geology, v. 24, p. 159-199.

Janecke, S.U., Perry, W. J., and M'Gonigle, J. W., 1996, Scale-development reactivation of pre-existing structures by an Eocene-Oligocene detachment fault, southwestern Montana: Geological Society of America Abstracts with Programs v. 28, p. 78.

Janecke, S.U., and Snee, L.W., 1993, Timing and episodicity of Middle Eocene volcanism and onset of conglomerate deposition, Idaho: Journal of Geology, v. 101, p. 603-621.

Janecke, S.U., Blankenau, J.J., VanDenburg, C.J., and Van Gosen, B.S., 2001, Normal faults and extensional folds of southwest Montana and eastern Idaho: Geometry, relative ages, and tectonic significance: U.S. Geological Survey Miscellaneous Field Studies 2362, scale 1:100,000.

Janecke, S.U., McIntosh, W., and Good, S., 1999, Testing models of rift basins: Structure and stratigraphy of a Eocene-Oligocene supra-detachment basin, Muddy Creek half graben, southwest Montana: Basin Research, v. 12, p. 143-167.

Janecke, S.U., VanDenburg, C.J., and Blankenau, J.J., 1998, Geometry, mechanisms, and significance of extensional folds from examples in the Rocky Mountain Basin and Range province, U.S.A.: Journal of Structural Geology, v. 20, p. 841-856.

Janecke, S.U., VanDenburg, C.J., Blankenau, J.C., and M'Gonigle, J.W., 2000, Long-distance longitudinal transport of gravel across the Cordilleran thrust-belt of Montana and Idaho: Geology, v. 28, p. 439-442.

Karlstrom K.E., Harlan, S.S., Williams, M.L., McLelland, G., Geissman, J.W., Ahall, K.I., 1999, Refining Rodinia; geologic evidence for the Australia-Western U.S. connection in the Proterozoic: GSA Today, v. 9, v. 1-7.

Kickham, J.C., 2002, Structural and kinematic evolution of the Eocene-Oligocene Grasshopper extensional basin, SW Montana [M.S. thesis]: Utah State University, 142 p.

Lindsey, D.A., 1972, Sedimentary petrology and paleocurrents of the Harebell Formation, Pinyon Conglomerate, and associated coarse clastic deposits, northwestern Wyoming: U.S. Geological Survey Professional Paper 734-B, 68 p.

Lund, K., Tysdal, R.G., Evans, K.V., and Winkler, G., 2003, Geologic map of the east half of the Salmon National Forest, in Evans, K.V., and Green, G.N., compilers., Geologic map of the Salmon National Forest and vicinity, east-central Idaho, U.S. Geological Survey Miscellaneous Investigations Map I-2765.

Matoush, J.P., 2002, The stratigraphic, sedimentologic, and paleogeographic evolution of the Eocene-Oligocene Grasshopper extensional basin, southwest Montana [M.S. thesis]: Utah State University, 188 p.

McClay, K.R., 1989, Physical models of structural styles during extension, *in* A.J., and Balkwill, H.R., eds., Extensional tectonics and stratigraphy of the North Atlantic margins, Tankard: American Association of Petroleum Geologists Memoir 46, p. 95-110.

McQuarrie, N., and Rodgers, D.W., 1998, Subsidence of a volcanic basin by flexure and lower crustal flow: The eastern Snake River Plain, Idaho: Tectonics, v. 17, p. 203-220.

M'Gonigle, J.W., and Dalrymple, G.B., 1993, $^{40}Ar/^{39}Ar$ ages of Challis volcanic rocks and the initiation of Tertiary sedimentary basins in southwestern Montana: Mountain Geologist, v. 30, p. 112-118.

M'Gonigle, J.W., and Dalrymple, G.B., 1996, $^{40}Ar/^{39}Ar$ ages of some Challis volcanic Group rocks and the initiation of Tertiary sedimentary basins in southwestern Montana: U.S. Geological Survey Bulletin 2132, 17 p.

M'Gonigle, J.W., Kirschbaum, M.A., and Weaver, J.N., 1991, Geologic map of the Hansen Ranch quadrangle, Beaverhead County, southwest Montana: U.S. Geological Survey Quadrangle Map GQ-1704, scale 1:24,000.

Moores, E.M., 1991, Southwest U.S.-East Antarctic (SWEAT)

connection; a hypothesis: Geology, v. 19, p. 425-428.

Nichols, R., Tabrum, A.R., and Hill, C.L., 2001, Cenozoic vertebrate paleontology and geology of southwestern Montana and adjacent areas, *in* Hill, C.L., ed., Mesozoic and Cenozoic Paleontology in the Western Plains and Rocky Mountains: Boseman, MT, Society of Vertebrate Paleontology 61st Annual Meeting, Guidebook, p. 79-110.

O'Neill, J.M., Lonn, J.D., and Kalakay, T.J., 2002, Early Tertiary Anaconda metamorphic core complex: Geological Society of America, Abstracts with Programs, v. 34, p. A-10.

Rodgers, D.W., and Janecke, S.U., 1992, Tertiary paleogeographic maps of the western Idaho-Wyoming-Montana thrust belt, *in* Link, P. K., Kuntz, M. A., and Platt, L. B., eds., Regional geology of eastern Idaho and western Wyoming: Geological Society of America Memoir 179, p. 83-94.

Ross, C.P., 1962, Stratified rocks in south-central Idaho: Idaho Bureau of Mines and Geology Pamphlet 125, 126 p.

Ross, C.P., 1963, Geology along U.S. Highway 93 in Idaho: Idaho Bureau of Mines and Geology Pamphlet 130, 80 p.

Ruppel, E.T., 1975, Precambrian and lower Ordovician rocks in east-central Idaho: U. S. Geological Survey Professional Paper 889, 34 p.

Ruppel, E.T., Lopez, D.A., and O'Neil, J.M., 1993, Geologic map of the Dillon 1° x 2° Quadrangle, Idaho and Montana: U.S. Geological Survey Miscellaneous Investigations I-1803-H, scale 1:250,000.

Ryder, R.T., and Scholten, R., 1973, Syntectonic conglomerates in southwestern Montana: Their nature, origin, and tectonic significance: Geological Society of America Bulletin, v. 84, p. 773-796.

Schlische, R.W., 1996, Geometry and origin of fault-related folds in extensional settings: American Association of Petroleum Geologists Bulletin, v. 79, p. 1661-1678.

Sears, J. W., and Fritz, W. J., 1998, Cenozoic tilt domains in southwestern Montana: Interference among three generations of extensional fault systems, *in* Faulds, J. E., and Stewart, J. H., eds., Accommodation zones and transfer zones: The regional segmentation of the Basin and Range province, Geological Society of America Special Paper 323, p. 241-249.

Sears, J.W., and Price R.A., 2000, New look at the Siberian connection; no SWEAT: Geology, v. 28, p. 423-426.

Skipp, B., 1987, Basement thrust sheets in the Clearwater orogenic zone, central Idaho and western Montana: Geology, v. 15, p. 220-224.

Staatz, M.H., 1979, Geology and Mineral Resources of the Lemhi Pass Thorium District, Idaho and Montana: U.S. Geological Survey Professional Paper 1049-A, 90 p.

Tucker, D.R., 1975, Stratigraphy and structure of Precambrian Y

(Belt?) metasedimentary rocks and associated rocks, Goldstone Mountains quadrangle, Lemhi County Idaho, and Beaverhead County, Montana [Ph.D. thesis]: Miami University, 245 p.

Tucker, D.R., 1983, Structural analysis of a detachment zone in east-central Idaho: Northwest Geology, v. 12, p. 57-62.

Tucker, D.R., and Birdseye, R.U., 1989, An Eocene synvolcanic alluvial fan complex in east-central Idaho: Stratigraphic relationships and structural implications: The Mountain Geologist, v. 6, p. 23-30.

Tysdal, R.G., 1996a, Geologic map of the Lem Peak quadrangle, Lemhi County, Idaho: U.S. Geological Survey Quadrangle Map GQ-1777, scale 1:24,000.

Tysdal, R.G., 1996b, Geologic map of adjacent areas in the Hayden Creek and Mogg Mountain quadrangles, Lemhi County, Idaho: U.S. Geological Survey Miscellaneous Investigations Series Map I-2563, scale 1:24,000.

Tysdal, R.G., and Moye, F.J., 1996, Geologic map of the Allison Creek quadrangle, Lemhi County, Idaho: U.S. Geological Survey Quadrangle Map GQ-1778, scale 1:24,000.

Tysdal, R.G., 2002, Structural geology of western part of Lemhi Range, east-central Idaho, U.S. Geological Survey Professional Paper 1659, 33 p.

VanDenburg, C.J., 1997, Tectonic and paleogeographic evolution of the Horse Prairie half graben, southwest Montana [M.S. thesis]: Utah State University, 152 p.

VanDenburg, C.J., Janecke, S.U. and McIntosh, W.C., 1998, Three-dimensional strain produced by >50m.y. of episodic extension, Horse Prairie rift basin, SW Montana, USA: Journal of Structural Geology, v. 20, p. 1747-1767.

Wolfe, J.A., and Wehr, W., 1987, Middle Eocene dicotyledonous plants from Republic northeastern Washington: U.S. Geological Survey Bulletin 1597, 25 p.

Xiao, H., and Suppe, J., 1992, Origin of rollover: American Association of Petroleum Geologists Bulletin, v. 76, p. 509-529.